Article

Not peer-reviewed version

Synthesis of Helional by Hydrodechlorination Reaction in the Presence of Mono and Bi-metallic Catalysts Supported on Alumina

Oreste Piccolo * , Iztok Arčon , Gangadhar Das , Giuliana Aquilante , Andrea Prai , Stefano Paganelli , Manuela Facchin , Valentina Beghetto

Posted Date: 26 January 2024

doi: 10.20944/preprints202401.1874.v1

Keywords: Helional®; selective hydrodechlorination; heterogeneous catalysis; XANES analysis; EXAFS analysis

Article

Synthesis of Helional by Hydrodechlorination Reaction in the Presence of Mono and Bi-Metallic Catalysts Supported on Alumina

Oreste Piccolo [1,*], Iztok Arčon [2,3], Gangadhar Das [4], Giuliana Aquilanti [4], Andrea Prai [5,†], Stefano Paganelli [5,6], Manuela Facchin [5] and Valentina Beghetto [5,6,7]

[1] Studio di consulenza scientifica (SCSOP), Via Bornò 5, 23896 Sirtori (LC), Italy*.
[2] University of Nova Gorica, Vipavska 13, SI-5000 Nova Gorica, Slovenia, iztok.arcon@ung.si
[3] Institute Jožef Stefan, SI-1000 Ljubljana, Slovenia
[4] Elettra, Sincrotrone Trieste, s.s. 14, km 163.5 34149 Basovizza, Trieste (Italy): giuliana.aquilanti@elettra.eu
[5] Università Ca' Foscari Venezia, Dipartimento di Scienze Molecolari e Nanosistemi, via Torino 155, 30172 Venezia Mestre (VE), Italy Andrea Prai 874116@stud.unive.it; spag@unive.it; manuela.facchin@unive.it; beghetto@unive.it
[6] Consorzio Interuniversitario Reattività Chimica e Catalisi (CIRCC), Via Celso Ulpiani 27, 70126 Bari, Italy
[7] Crossing S.r.l., Viale della Repubblica 193/b, 31100, Treviso, Italy valentina.beghetto@crossing-srl.com
[*] Correspondence: orestepiccolo@tin.it ; Tel.: +39-3939479870.
[†] Present address: andrea.prai@studenti.unime.it.

Abstract: Hydrodechlorination reaction of 3-(benzo-1,3-dioxol-5-yl)-3-chloro-2-methylacrylaldehyde in the presence of different low metal content heterogeneous mono- or bi-metallic catalysts was tested for the synthesis of the fragrance Helional® (3-[3,4-methylendioxyphenyl]-2-methyl-propionaldehyde). In particular, mono Pd/Al_2O_3, Rh/Al_2O_3 or bi-metallic Pd-Cu/Al_2O_3, Rh-Cu/Al_2O_3 catalysts were tested in different reaction conditions from which it emerged that mono-Rh/Al_2O_3 was the best performing catalyst allowing to achieve 100% substrate conversion and 99% selectivity towards Helional® in 24h at 80°C, p(H_2) 1.0 MPa in the presence of a base. To establish correlations between atomic structure and catalytic activity, catalysts were characterized by Cu, Rh and Pd K-edge XANES, EXAFS analysis. These characterizations allowed to verify that the formation of Pd-Cu alloys and the presence of Cu oxide/hydroxide species on the surface of the Al_2O_3 support, are responsible for the very low catalytic efficiency of bimetallic species tested.

Keywords: Helional®; selective hydrodechlorination; heterogeneous catalysis; XANES analysis; EXAFS analysis

1. Introduction

Many heterogeneous catalysts are commercially available on the market but their performances, in terms of selectivity, activity, stability and cost, are often unsatisfactory or unsustainable [1–4]. To find a suitable catalyst for a specific process, fulfilling all the desired characteristics remains a challenging task [2,3,5]. When heterogeneous catalysts are employed, metal leaching or poisoning may sometimes occur, making the catalyst recyclability impossible [6–10]. In particular, when fine chemicals are prepared, catalyst leaching implies further costly purification steps to reduce to authorised levels the presence of metal contamination. Many procedures have been developed to overcome these drawbacks and to obtain efficient heterogeneous catalysts [11,12], among which impregnation of metals on a support is one of the simplest and most commonly employed protocols. Metallic species are dispersed on a pre-dried support by incipient wetness impregnation techniques in aqueous or non-aqueous solution [13–15], followed by calcination and activation [16–18]. Milder and less energy consuming preparation methods are relevant targets in catalysts development, possibly avoiding the use of water to limit metal leaching. An interesting example has been reported in a patent by Piccolo and coworkers describing a simple and efficient protocol for the preparation, at industrial scale, of a heterogeneous rhodium catalyst with very low catalyst loading (0.18%

Rh/Al_2O_3). This catalyst proved to be very active for the selective hydrogenation of alpha-beta-unsaturated carbonyl compounds [19]. The catalyst, prepared in tetrahydrofuran (THF), or in the greener cyclopentyl methyl ether (CPME), at very low concentrations, also showed excellent activity, in terms of selectivity and recyclability, in the hydrogenation and/or hydroformylation of other C=C and C≡C bond, with no catalyst leaching [20]. As far as the synthesis of fine chemicals is concerned, Rh/Al_2O_3 but also Pd/Al_2O_3 and bi-metallic $Pd\text{-}Cu/Al_2O_3$ catalysts have been demonstrated to be very active and selective in the semi hydrogenation of 3-hexyn-1-ol to (*Z*)-3-hexen-1-ol, a particularly important fragrance with an herbaceous note [21] and in the synthesis of aryl and heteroaryl aldehydes via reductive carbonylation [22,23].

Focusing on the synthesis of fine chemicals, we deemed it interesting to evaluate the efficiency of these heterogeneous catalysts for the preparation of Helional® (3-[3,4-methylendioxyphenyl]-2-methyl-propionaldehyde). Helional® is a high added-value fragrance employed in its racemic form in many perfumes for its green, floral (cyclamen) and marine fresh note, prepared at industrial level by different strategies (Scheme 1). Specifically, Helional® is mainly prepared by crossed-aldol condensation between heliotropin (5-carboxyaldehyde-1,3-benzodioxol) (**I**), that is now a controlled substance, and propanal to obtain (**II**), followed by selective hydrogenation of the intermediate alkene formed (Scheme 1a) [24,25]. However, this methodology has a series of disadvantages, such as for example the fact that yields above 50-55% may not be achieved in the aldol condensation due to self-condensation of propionaldehyde and the reaction of this latter with (**II**), requiring costly purification steps to separate by-products from (**III**). Alternative methods foresee the synthesis of Helional® starting from the alkylation of 1,2-methylenedioxybenzene (MDB) (**IV**) with 2-methylprop-2-ene-1,1-diyl diacetate (**V**), followed by hydrolysis of 1-acetoxy-2-methyl-3-(3,4-methylendioxyphenyl)propene) (**VI**) to give the corresponding unsaturated aldehyde, which is then reduced to give the desired product (**III**) (Scheme 1b) [8,26]. Synthetic strategies above reported suffer of further drawbacks such as the use of expensive or difficult to handle catalysts, the use of Lewis acids, the use of expensive reagents such as methacrolein diacetate (**V**).

An interesting alternative has been reported by Borzatta and coworkers starting from cheap and easily available 5-propanoyl-1,3-benzodioxol (**VII**). **VII** is reacted with the Vilsmeier reagent (1-chloro-N,N-dimethylmethaniminium chloride) (**VIII**) at temperatures ranging between 0-40°C to obtain the unsaturated chloroaldehyde 3-(benzo-1,3-dioxol-5-yl)-3-chloro-2-methylacrylaldehyde (**IX**), which is then hydrodechlorinated to give (**III**) in the presence of 5% Pd/C and an organic or inorganic base (Scheme 1c) [12].

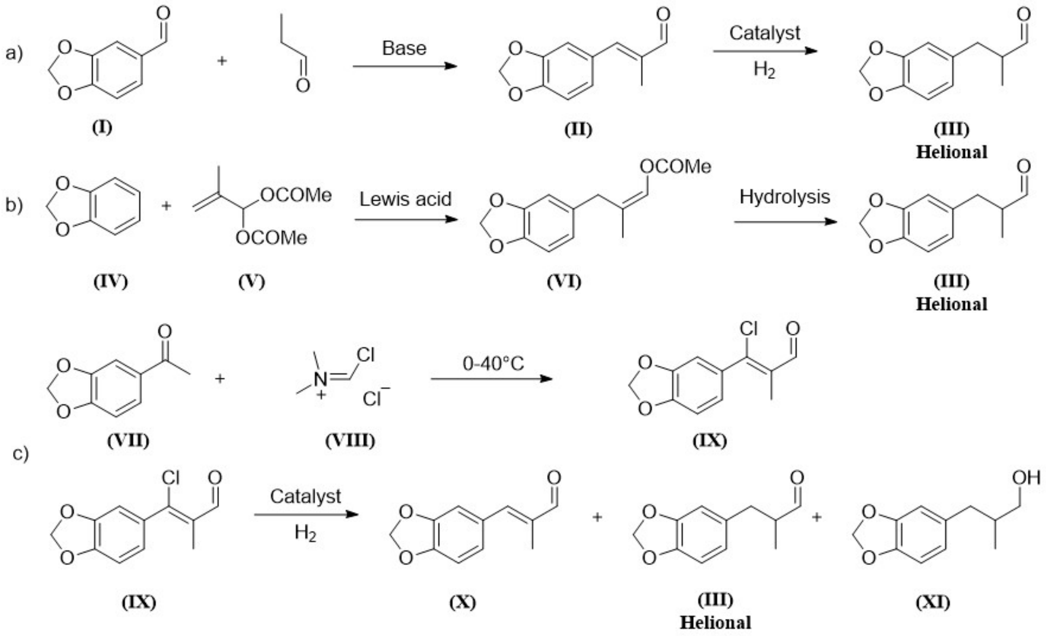

Scheme 1. Main protocols for the synthesis of Helional® (**III**).

Within this panorama, the possibility to employ low metal content heterogeneous catalysts reported by Piccolo and collaborators for the selective hydrodechlorination of α,β-unsaturated aldehydes such as (**IX**) appeared very challenging also for industrial applications [27–32].

Thus, in this paper the hydrodechlorination reaction of 3-(benzo-1,3-dioxol-5-yl)-3-chloro-2-methylacrylaldehyde (**IX**), for the selective synthesis of Helional® (**III**), has been reported in the presence of different low metal content heterogeneous mono-Pd/Al_2O_3 or Rh/Al_2O_3 and bi-metallic $Pd\text{-}Cu/Al_2O_3$, $Rh\text{-}Cu/Al_2O_3$ catalysts. Moreover, all catalysts tested were characterised by XANES and EXAFS before and after the hydrodechlorination reaction.

2. Results

The catalytic activity of the mono-Pd or Rh supported on Al_2O_3 and bi-metallic $Pd\text{-}Cu/Al_2O_3$ or $Rh\text{-}Cu/Al_2O_3$ species were tested in different reaction conditions for the hydrodechlorination of 3-(benzo-1,3-dioxol-5-yl)-3-chloro-2-methylacrylaldehyde (IX) and data are reported below (Tables 1 and 2). The use of bimetallic species was investigated since $Pd\text{-}Cu/Al_2O_3$ or $Rh\text{-}Cu/Al_2O_3$ catalysts would allow to reduce the quantity of transition metal employed and consequently industrial costs.

Table 1. Hydrodechlorination of (IX) catalyzed by 0.3% Pd/Al_2O_3, or $Pd\text{-}Cu/Al_2O_3$ (0.18% Pd, 0.43% Cu) in the presence of different bases.

Run	Catalyst	Base	t (h)	Conv. (%)[a]	(X) (%)[a]	(III) (%)[a]	(XI) (%)[a]
1	Pd/Al_2O_3	Na_2CO_3	6	65	15	49	1
2		Na_2CO_3	24	98	3	74	21
3		TOA	6	81	6	56	19
4		TOA	24	95	3	62	30
5		TEA	6	88	11	72	5
6		TEA	24	100	1	83	16
7	$Pd\text{-}Cu/Al_2O_3$	TEA	6	7	3	4	n.d.
8		TEA	24	12	5	6	1
9[b]		TEA	6	29	6	20	3
10[b]		TEA	24	50	5	40	5

Reaction conditions: Substrate (**IX**): 20 mg (8.9×10^{-2} mmol); Catalyst: 0.3% Pd/Al_2O_3, 3.7 mg (8.9×10^{-5} mmol); (**I**)/Metal molar ratio: 1000/1; Solvent: 2-propanol (5 mL); T: 80°C; $p(H_2)$: 0.5 MPa; Base: 2 equivalents. a Determined by GLC analysis in the presence of 8.9×10^{-3} mmol of isopropyl benzene as internal standard. b $p(H_2)$: 1.0 MPa.

Table 2. Hydrodechlorination of (IX) catalyzed by 0.18% Rh/Al_2O_3 or $Rh\text{-}Cu/Al_2O_3$ (0.19% Rh, 0.8% Cu) in the presence of different bases.

Run	Catalyst	Base	$p(H_2)$ (MPa)	t (h)	Conv.[a] (%)	(X) (%)[a]	(III) (%)[a]	(XI) (%)[a]
1	Rh/Al_2O_3	Na_2CO_3	0.5	6	67	25	41	1
2		Na_2CO_3	0.5	24	85	3	72	10
3		Na_2CO_3	1.0	6	75	18	57	n.d.
4		TEA	1.0	24	100	1	99	n.d.
5	$Rh\text{-}Cu/Al_2O_3$	TEA	1.0	4	23	14	9	n.d.
6		TEA	1.0	16	43	12	28	3
7		TEA	1.0	24	68	9	51	8

Reaction conditions: Substrate (**IX**): 8.9×10^{-2} mmol; Catalyst: 8.9×10^{-5} mmol; (**I**)/Metal molar ratio: 1000/1; Solvent: 2-propanol (5 mL); T: 80°C; Base: 2 equivalents. a Determined by GLC analysis in the presence of 8.9×10^{-3} mmol of isopropyl benzene as internal standard.

2.1. Catalytic hydrodechlorination of 3-(benzo1,3-dioxol-5-yl)-3-chloro-2-methylacrylaldehyde (IX)

Preliminary experiments were carried out to verify the efficiency of mono- and bimetallic Pd based supported catalysts containing 0.3% or 0.18% quantities of transition metal. Since the hydrodechlorination of (**IX**) leads to the formation of hydrochloric acid, first experiments were devoted to highlight the influence of different inorganic and organic bases (Na_2CO_3, trioctyl amine (TOA) and triethyl amine (TEA)) on the catalyst efficiency, and relevant data are reported in Table 1. Unless otherwise stated, reactions were carried out with a substrate/metal molar ratio of 1000/1 at 80 °C and 0.5 MPa p(H_2), in the presence of 2 equivalents of a base. Data reported in Table 1 are the mean values of at least three experiments.

After 6 hours at 80°C, in the presence of Na_2CO_3, the conversion was rather low (65%) and selectivity to (**III**) around 75%, with the formation of both the unsaturated product 3-(1,3-benzodioxol-5-yil)-2-methyl-propenal (**X**) (15%) and 3-(1,3-benzodioxol-5-yil)-2-methyl-propanol (**XI**) (1%) (run 1, Table 1). Increasing the reaction time to 24 h strongly increased substrate conversion (98%) although selectivity to (**III**) was almost equivalent to that achieved by 6h (78%, compare runs 1 and 2) and the formation of alcohol (**XI**) also increased (run 2, Table 1). To verify if higher catalyst efficiency could be achieved substituting Na_2CO_3, insoluble in the reaction mixture, with a soluble organic base, further experiments were carried out in the presence of TOA or TEA [21,23]. According to data reported in Table 1 it emerges that TOA gave no significant improvement as compared to Na_2CO_3 (compare runs 1-4, Table 1), while in the presence of less hindered TEA best results were obtained, affording 100% conversion of (**IX**) and 83% selectivity to (**III**) by 24h (compare runs 3-6, Table 1).

Encouraged by the good results obtained with Pd/Al_2O_3, the activity of the bi-metallic Pd-Cu/Al_2O_3 (0.18% Pd, 0.43% Cu) catalyst was also investigated. In the same reaction conditions employed with Pd/Al_2O_3, the bimetallic specie gave very unsatisfactory results (runs 7-10, Table 1). At best, Helional® (**III**) was obtained in 40% selectivity after 24h at 1.0 MPa of hydrogen pressure (run 10, Table 1). This result was completely unexpected and surprising given the excellent results obtained with this bimetallic catalyst in reductive carbonylation reactions for the synthesis of aldehydes [7]. As a matter of fact, when the bimetallic system Pd-Cu/Al_2O_3 was used, the activity of the catalyst was very high, probably due to a synergic effect of the two metals. Even the only copper-based catalyst 1% Cu/Al_2O_3, although it does not contain any precious metal, gave excellent conversions and aldehyde yields. Unfortunately, when 1% Cu/Al_2O_3 was used in the hydrodechlorination of (**IX**) conversion was practically negligible (data not reported in the table). A possible explanation for this different behaviour may be attributable, in the hydrodechlorination but not in the carbonylation process, to the formation of alloys that reduce the amount of active catalyst and to the presence of catalytically not active Cu(II) oxide/hydroxide species on the surface of the Al_2O_3 support (see discussion section).

Alternatively, 0.18% Rh/Al_2O_3 was tested for the catalytic hydrodechlorination of (**IX**), and results are reported in Table 2. In the same reaction conditions employed in the presence of 0.3% Pd/Al_2O_3 (run1, Table 1), Rh/Al_2O_3 gave comparable results (run 1, Table 2).

Moreover, increasing hydrogen pressure to 1.0 MPa, in the presence of 2 equivalents TEA, allowed to achieve total conversion of (**IX**), with almost complete selectivity to (**III**) by 24h (99%) (run 4, Table 2). Interestingly, no total hydrogenation by-product (**XI**) was detected in the reaction crude.

Finally, the activity of the bimetallic Rh-Cu/Al_2O_3 catalyst (0.19% Rh, 0.8% Cu) was also evaluated. Nevertheless, as for bi-metallic Pd-Cu/Al_2O_3 species, also Rh-Cu/Al_2O_3 based catalyst showed very lower performances compared to Rh/Al_2O_3 (entries 5-7, Table 2). Also in this case, catalytically not active Cu(II) oxide/hydroxide species are present on the surface of Al_2O_3 so hindering the performance of the Rh active sites (see discussion section).

To gain further understanding on the nature of the catalysts and on the very low efficiency of bimetallic species, Pd/Al_2O_3, Rh/Al_2O_3, Cu/Al_2O_3, Pd-Cu/Al_2O_3 and Rh-Cu/Al_2O_3 were characterised, before and after catalytic reactions, by XANES and EXAFS (see supplementary materials).

3. Discussion

The Cu, Rh and Pd K-edge XANES were used to monitor the valence state and local symmetry of Cu, Rh and Pd cations in the Cu/Al_2O_3, Pd/Al_2O_3 Pd-Cu/Al_2O_3, Rh/Al_2O_3 and Rh-Cu/Al_2O_3 catalysts before and after the catalytic reaction. Different local environments of the investigated cation result in different K-edge profiles in the XANES spectra [13–19]. Further, the Cu, Rh and Pd K-edge EXAFS were used to determine the average local neighbourhood of Cu, Rh and Pd cations in the Cu/Al_2O_3, Rh-Cu/Al_2O_3 and Pd-Cu/Al_2O_3 catalyst in the initial state and in the final state, after catalytic reaction. The analysis of the EXAFS spectra was performed with the Demeter (IFFEFIT) program package [20] in combination with the FEFF6 program code [21] for *ab initio* calculation of photoelectron scattering paths. Structural parameters of the average local Cu, Rh and Pd neighbourhood (type and average number of neighbours, the radii and Debye-Waller factor of neighbour shells) are quantitatively resolved from the EXAFS spectra by comparing the measured EXAFS signal with model signal. Combined FEFF models are used, composed of neighbour atoms at distances characteristic for the expected Cu, Rh and Pd oxide and metal species that may be present in the samples in the initial or final state, or after catalytic reaction. The atomic species of neighbours are identified in the fit by their specific scattering factor and phase shift. Details of the XANES and EXAFS analyses are presented in the supplementary materials.

The Cu K-edge XANES results (Table S1) show that monometallic Cu/Al_2O_3, catalyst contains only Cu(II) cations octahedrally coordinated to oxygen atoms. The Cu valence state and local symmetry does not change during the catalytic reaction. Bimetallic Rh-Cu/Al_2O_3 catalyst also contains only Cu(II) species with the same local symmetry, however during the catalytic reaction 15% of Cu cations are reduced to metallic form. Bimetallic Pd-Cu/Al_2O_3 catalyst contains a mixture of Cu cations in three valence states, 54% of Cu(II), 4% of Cu(I) and 42% of metallic Cu. During catalytic reaction relative amounts of Cu(II) and Cu(I) species increased and relative amount of metallic Cu decreased.

The Cu EXAFS results (Table S2) show that Cu cations in monometallic Cu/Al_2O_3 and bimetallic Rh-Cu/Al_2O_3 catalyst in the initial state are coordinated with six oxygen atoms in the first coordination shell at two different distances, and Al and Cu are neighbours in more distant coordination shells. The distances to oxygen and Cu neighbours are characteristic for the local structures of Cu cations in Cu oxide/hydroxide species [14,15] indicating that the samples contain a mixture of copper oxide/hydroxide species, in agreement with the Cu K-edge XANES result. The presence of two Al neighbours at about 3.1 Å clearly indicates that part of the Cu cations is directly attached to the Al_2O_3 framework forming Cu–O–Al bridges. So, it is possible to conclude that the Cu(II) oxide/hydroxide species are highly dispersed on the Al_2O_3 support and tightly attached to its surface. During the catalytic reaction the average structure of Cu oxide/hydroxide species in the monometallic Cu/Al_2O_3 is preserved. However, average number of Al neighbours is significantly decreased, which indicates that about half of Cu–O–Al bridges are lost during the catalytic reaction.

In the bimetallic Rh-Cu/Al_2O_3 catalyst the local structure around Cu cations changes significantly during the catalytic reaction. Part of Cu cations is reduced to metallic form, as already indicated by Cu XANES analysis, and form small Cu metallic nanoparticles with fcc crystal structure. The remaining part of Cu cations remains in the form of Cu(II) oxide/hydroxide species, but the Cu–O–Al bridges are lost.

The bimetallic Pd-Cu/Al_2O_3 catalyst contains a mixture of Cu metal nanoparticles with fcc crystal structure and Cu oxide/hydroxide species already present in the initial state, in agreement with the Cu K-edge XANES results. There are no Al neighbours in the second coordination shell, which indicates that there are no Cu–O–Al bridges present in the sample, or that their amount is below the detection limit. During the catalytic reaction the average local structure around Cu cations is mainly preserved. Only the coordination number of Cu neighbours in the second coordination shell in the metal fcc structure is significantly increased, indicating that average size of Cu metal nanoparticles is increased, and according to the Cu K-edge XANES results, the relative amount of Cu metal species is slightly decreased.

The Rh K-edge XANES analysis of the Rh/Al_2O_3 and Rh-Cu/Al_2O_3 catalyst in the initial state and in the final state after catalytic reaction indicate that the catalysts contain predominantly Rh oxide species and a small amount of Rh in the metallic form (Table S3). Relative amounts of metallic Rh species in the catalysts increase significantly during the catalytic reaction. The Rh EXAFS analysis (Table S4) shows that in all four samples Rh cations are coordinated to oxygen neighbours at the distance of 2.03 Å, characteristic for Rh oxide, and Rh neighbours at 2.67 Å, characteristic for the nearest coordination shell in Rh metal. In the fresh monometallic Rh/Al_2O_3 sample, 4 oxygen atoms and only about 0.6 Rh neighbours were present, indicating that the sample contains predominantly Rh oxide species with about 10% of Rh in the metallic form. After the catalytic reaction the average number of oxygen neighbours decreased to about 3 and the number of Rh neighbours increased to about 2. These results indicate that part of Rh oxide species is reduced to metallic form and relative amount of Rh metal species increased during the catalytic reaction. Same process was observed also for the bimetallic Rh-Cu/Al_2O_3 catalyst. After the catalytic reaction, the average number of oxygen neighbours decreased from 4 to about 2.5 and average number of Rh neighbours increased from 1 to about 5, indicating that even higher amounts of Rh oxide species are reduced to the metallic form. The Rh EXAFS results are consistent with the Rh XANES results.

The Pd K-edeg XANES analysis of the Pd/Al_2O_3 and Pd-Cu/Al_2O_3 catalyst in the initial state and in the final state after catalytic reaction (Figure S6) indicate that the catalysts contain predominantly Pd cations in the metal form. The Pd EXAFS results (Table S5) reveal that fresh monometallic Pd/Al_2O_3 catalyst contains predominantly metallic Pd in the form of small Pd metal nanoparticles with fcc crystal structure and a small amount of Pd oxide species. During the catalytic reaction the average local structure around Pd cations changes, since the coordination number of Pd neighbours in more distant coordination shells in the metal fcc structure is significantly increased, indicating that average size of Pd metal nanoparticles also increased. On the contrary the coordination numbers of oxygen and Pd neighbours of Pd oxide species significantly decreased and shifted to lower distances, indicating the formation of smaller Pd oxide nanoparticles.

The bimetallic Pd-Cu/Al_2O_3 catalysts exhibit significantly different local structure around Pd cations compared to the monometallic Pd/Al_2O_3 catalyst. In the local Pd neighbourhood there are in average two Cu neighbours at the distance of 2.58 Å and seven Pd neighbours at the distance of 2.70 Å. The Pd-Cu and Pd-Pd distances are in perfect agreement with those reported for the Pd-Cu metal nanoparticles [31]. The fresh bimetallic Pd-Cu/Al_2O_3 catalyst contains predominantly Pd-Cu metal alloy nanoparticles and a small amount of Pd oxide species. After the catalytic reaction the average coordination numbers of Cu and Pd neighbours are increased, indicating that average size of Pd-Cu metal nanoparticles increased. Surprisingly, for Pd-Cu/Al_2O_3 sample, Cu-Pd alloy nanoparticles were formed [6], while for Cu and Rh catalyst, no Cu-Rh alloy was formed. The two metals remained separated in similar nanoparticles as in the corresponding monometallic catalysts.

4. Materials and Methods

All reagents and solvent were purchased from Aldrich and used as received. γ-Al_2O_3 was a generous gift of Chimet S.P.A. (Italy) while 1-(benzo1,3-dioxol-5-yl)propan-1-one was a generous gift of Endura S.P.A.(Italy). Helional® was synthetized according to the literature [12]. 0.3% Pd/Al_2O_3, 1% Cu/Al_2O_3, 0.18% Rh/Al_2O_3, (0.18% Pd, 0.43% Cu)/Al_2O_3 and (0.19% Rh, 0.8% Cu)/Al_2O_3 were prepared in a one pot procedure following literature procedures [20–23]. In all cases, a stirred mixture of the metal precursor, trioctyl amine (TOA) and alumina type 49 in cyclopentyl methyl ether (CPME) was heated under hydrogen pressure. The grey solid obtained was filtered under nitrogen, washed with CPME and with n-hexane and then dried under vacuum. The metal content was determined by atomic absorption measurements using a Perkin Elmer Analyst 100 spectrometer equipped with a single-element hollow cathode lamp. GLC analyses were carried out with an Agilent 6850A equipped with a Free Fatty Acid capillary column and using isopropyl benzene as internal standard. GC-MS analyses were performed with an Agilent 7820A GC System coupled with quadrupole mass spectrometer Agilent 5977B MSD equipped with a HP-5MS capillary column. Organic products were characterised by ^1H NMR spectra recorded in $CDCl_3$ solutions with a Bruker Avance 400 spectrometer working at 400 MHz, and data compared to literature ones [12,35,36]. Cu, Rh and Pd K-edge XANES and EXAFS spectra were measured in transmission detection mode. The experiments were performed at the XAFS beamline of the Elettra synchrotron in Trieste, Italy [37]. Further details are reported in the supporting information.

4.1. Synthesis of 3-(benzo1,3-dioxol-5-yl)-3-chloro-2-methylacrylaldehyde (IX)

The synthesis of (**IX**) was carried out according to the literature [12]. 20.5 g of *N,N*-dimethylformamide at 0°C were introduced in a jacketed 3-necked flask equipped with a bubble condenser and then 23 g of $POCl_3$ were added under an inert atmosphere. The mixture was left to react for 2 hours after which the temperature was raised to 20°C for 30 minutes. Once the temperature was reached, a solution of 14.3 g of 1-(benzo-1,3-dioxol-5-yl)propan-1-one in *N,N*-dimethylformamide was added over a period of approximately 4 h and left to react overnight at 35°C. The mixture was cooled to 10°C, then 35 g of toluene and 95 g of a 3M NaOH solution were added in 3 h, at controlled temperature (20°C) and for further 2h at 25°C. The organic phase was collected and solvent evaporated to give a mixture containing 99.3% of 3-(benzo-1,3-dioxol-5-yl)-3-chloro-2-methylacrylaldehyde (**IX**) and 0.7% 1-(benzo-1,3-dioxol-5-yl)propane as confirmed by GC-MS m/z 3-(benzo1,3-dioxol-5-yl)-3-chloro-2-methylacrylaldehyde (**I**): 224[M]$^+$, 189[M-Cl]$^+$, 161[M-Cl- CO]$^+$. ^{1}H NMR (400 MHz, $CDCl_3$) δ 9.51 (s, 1H), 6.94 (s, 1H), 6.83 (m, 2H), 6.05 (s, 2H), 5.98 (s, 1H).

4.2. General procedure for the hydrodechlorination of 3-(benzo-1,3-dioxol-5-yl)-3-chloro-2-methylacrylaldehyde (IX)

In a Schlenk tube equipped with a magnetic stirring bar, under inert atmosphere, 20 mg (8.9×10^{-2} mmol) of (**IX**), 5 mL of 2-propanol, 2 equivalents of a base, 8.9×10^{-3} mmol of isopropyl benzene as internal standard and the catalyst were added in the desired amount. The Schlenk tube was then transferred into a 150 mL stainless steel autoclave under nitrogen, pressurized with hydrogen at the desired pressure and heated at 80°C for 6h or 24h, under stirring. The reactor was then cooled to room temperature and the residual gases vented off. The reaction mixture was centrifuged, and the organic solution analysed by GLC and GC-MS. All data were performed in triplicates and average values are reported in Tables 1 and 2 (see Section 2).

GC-MS m/z (*E*)-3-(benzo-1,3-dioxol-5-yl)-2-methylacrylaldehyde (**X**): 190 [M]$^+$; 175 [M-CH_3]$^+$; 161 [M-CHO]$^+$. GC-MS m/z 3-(benzo-1,3-dioxol-5-yl)-2-methylpropanal (Helional®) (**III**): 192 [M]$^+$; 164 [M-CO]$^+$; 135 [M-CO-C_2H_4]$^+$; 121 [M-CO-C_2H_4-CH]$^+$. GC-MS m/z 3-(benzo-1,3-dioxol-5-yl)-2-methylpropan-1-ol (**XI**): 194[M]$^+$; 176[M-H_2O]$^+$; 135[M-CH_3-CH-CH_2OH]$^+$.

5. Conclusions

In this paper different mono and bimetallic heterogeneous catalysts have been tested for the synthesis of Helional (**III**) by hydrodechlorination of 3-(benzo-1,3-dioxol-5-yl)-3-chloro-2-methylacrylaldehyde (**IX**). In particular, Pd/Al_2O_3 and Rh/Al_2O_3 catalysts with low metal loadings (0.3% and 0.18%, respectively) were very efficient, reaching complete substrate conversion. In the presence of Pd/Al_2O_3 selectivity to (**III**) up to 83% were obtained in the presence of 2 equivalents of TEA, at 80°C, p(H_2) 0.5 MPa by 24h. When Rh/Al_2O_3 was chosen as catalyst, although a higher p(H_2) (1.0 MPa) was employed, total conversion of (**IX**) and very high selectivities to (**4**) (99%) were achieved by 24h, thus giving better results in comparison with data reported in the literature [12]. Hydrodechlorination tests carried out in the presence of bi-metallic Pd-Cu/Al_2O_3 and Rh-Cu/Al_2O_3 catalysts, showed that these catalysts have very lower performances compared to monometallic Pd/Al_2O_3 and Rh/Al_2O_3 catalysts.

To investigate the possible correlation between the atomic structure of the catalysts and the chemical state and atomic structure of the Cu, Rh and Pd cations on the alumina support, all the catalytic systems have been characterized by Cu, Rh and Pd K-edge XANES, EXAFS analysis.

The bimetallic Pd-Cu/Al_2O_3 catalysts exhibit significantly different local structure around Pd cations compared to the monometallic Pd/Al_2O_3 catalyst. The monometallic Pd/Al_2O_3 catalyst contains predominantly metallic Pd in the form of small Pd metal nanoparticles with fcc crystal structure while bimetallic Pd-Cu/Al_2O_3 catalysts contain predominantly Pd-Cu metal alloy nanoparticles, hindering the catalytic activity of Pd cations. In fact, from these characterisations it emerged that addition of Cu reduces the amount of catalytically active Pd sites by formation of Pd-Cu alloy nanoparticles. Additionally, the excess of Cu cations forms on alumina surface a mixture of Cu metal nanoparticles with fcc crystal structure and Cu oxide/hydroxide nanoparticles, which are catalytically not active.

In case of Rh based catalysts both the monometallic Rh/Al_2O_3 and bi-metallic Rh-Cu/Al_2O_3 contain Rh cations predominantly in the form of Rh oxide species and a small amount of metallic Rh. The main structural difference in the bi-metallic catalyst is represented by the presence Cu(II) oxide/hydroxide species highly dispersed and tightly attached on the surface of Al_2O_3. As for Pd-Cu/Al_2O_3, the Cu species are catalytically not active, and thus hinder the performance of the Rh active sites present on the surface of the Al_2O_3 support.

The XANES and EXAFS analysis also revealed structural changes and degradation of the catalyst after use, diminishing their catalytic performances. In case of the monometallic Rh/Al_2O_3 and bimetallic Rh-Cu/Al_2O_3 the reason can be attribute to nanoparticles formation and loss of the direct tight connection of the remaining Cu(II) oxide/hydroxide species to the alumina support. In case of the mono-metallic Pd/Al_2O_3 and bi-metallic Pd-Cu/Al_2O_3 catalyst the average size of Pd and Pd-Cu metal nanoparticles, increased during the catalytic reaction, decreasing the catalyst efficiency. Studies are ongoing to gain deeper insight into the different behaviour of mono and bimetallic catalysts and the role of alloys formed during the reaction.

Supplementary Materials: The following supporting information can be downloaded at the website of this paper posted on Preprints.org.

Author Contributions: A. P.: data curation, analysis and investigation in batches; I.A, G.A,.: data curation, analysis and investigation in XAFS and XANEX, evaluation of the text; S.P: methodology, investigation, evaluation of the text; M.F. : writing—review and editing; O.P.: conceptualization, methodology, investigation, data curation, supervision, validation, V.B.: writing—original draft preparation, writing—review and editing. All authors have read and agreed to the published version of the manuscript.

Funding: This research was funded by the Slovenian Research Agency (research core funding No. P1-0112) and access to synchrotron radiation facilities (XAFS beamline, project 20215267) of ELETTRA.

Data Availability Statement: The data presented in this study are available in the present article.

Acknowledgments: We thank Gangadhar Das and Ricardo Grisonich from XAFS beamline, for the assistance during experiment and expert advice on beamline operation.

Conflicts of Interest: The authors declare no conflict of interest.

References

1. Bartolomew, C.H.; Farrauto, R.J. Fundamentals of industrial catalytic processes, **2006**, 2nd ed. John Wiley and Sons, Hoboken.
2. Piccolo, O.; Verrazzani, A. Preparation and use of a heterogeneous rhodium catalyst for the hydrogenation of a double bond of an alpha-beta-unsaturated carbonyl compound. Patent No. US 7087548, (Chemi SpA), **2006**.
3. Paganelli, S.; Tassini, R.; Rathod, V.D.; Onida, B.; Fiorilli, S.; Piccolo, O. A low rhodium content smart catalyst for hydrogenation and hydroformylation reactions. *Catal. Lett.* **2021**, *151*, 1508-1521.
4. Paganelli, S.; Angi, A.; Pajer, N.; Piccolo, O. A smart heterogeneous catalyst for efficient, chemo- and stereoselective hydrogenation of 3-hexyn-1-ol. *Catalysts* **2021**, *11*, 14.
5. Scrivanti, A.; Sole, R.; Bortoluzzi, M.; Beghetto, V.; Bardella, N.; Dolmella, A.; Synthesis of new triazolyl-oxazoline chiral ligands and study of their coordination to Pd(II) metal centres, *Inorg. Chim. Acta* **2019**, *498*, 119129.
6. Paganelli, S.; Tassini, R.; Piccolo, O. Sustainable synthesis of aryl and heteroaryl aldehydes. *Chem. Select* **2022**, *7*, e202202393.
7. Bosello, N.; Di Michele, A.; Piccolo, O.; Paganelli, S. CO and H_2 gas-free efficient reductive carbonylation of aryl iodides. Use of smart recyclable metal-based catalysts, *Appl. Catal. A Gen.* **2023**, *657*, 119145.

8. Kraft, P.; Bajgrowicz, J.A.; Denis, C.; Frater, G. Odds and Trends: Recent Developments in the Chemistry of Odorants. *Angew. Chem. Int. Ed.* **2000**, *39*, 2980-3010.
9. Sole, R.; Buranello, C.; Bardella, N.; Di Michele, A.; Paganelli, S.; Beghetto, V.; Recyclable Ir nanoparticles for the catalytic hydrogenation of biomass-derived carbonyl compounds, *Catalysts* **2021**, *11*, 914.
10. Yang, V.; Vogler, B.; Lei, Y.; Wu, T. Metallic ion leaching from heterogeneous catalysts: an overlooked effect in the study of catalytic ozonation processes. *Environ. Sci.: Water Res. Technol*. **2017**, *3*, 1143-1151
11. Enders, D.; Backes, M. First asymmetric synthesis of both enantiomers of Tropional® and their olfactory evaluation. *Tetrahedron: Asymmetry* **2004**, *15*, 1813-1817.
12. Borzatta, V.; Capparella, E.; Poluzzi, E. Process for the preparation fo 3-(3,4-methylenedioxyphenyl)-2-methylpropanal. WO2005/105774 A1 (Endura S.p.a.), **2005**.
13. Arčon, I.; Paganelli, S.; Piccolo, O.; Gallo, M.; Vogel-Mikuš, K.; Baldi, F. XAS analysis of iron and palladium bonded to a polysaccharide produced anaerobically by a strain of Klebsiella Oxytoca. *J. Synchrotron Radiat*. **2015**, *22*, 1215.
14. Arčon, I.; Piccolo, O.; Paganelli, S.; Baldi, F. XAS analysis of a nanostructured iron polysaccharide produced anaerobically by a strain of Klebsiella Oxytoca. *Biometals* **2012**, *25*, 875-881.
15. Piccolo, O.; Paganelli, S.; Zanatta, P.; Tieuli, S.; Sperni, L.; Baldi, F.; Gallo, M.; Arčon, I.; Vogel-Mikuš, K. A biogenerated polymetallic catalyst from society's wastes. *Chem. Sci. Inter. J.* **2019**, *27*, 1-12.
16. Tieuli, S.; Baldi, F.; Arčon, I.; Vogel-Mikuš, K.; Gallo, M.; Sperni, L.; Piccolo, O.; Paganelli, S. Alternative recovery and valorization of metals from exhausted catalytic converters in a new smart polymetallic catalyst. *Chem. Select* **2019**, *4*, 4624-4632.
17. Zabilskiy, M.; Arčon, I.; Djinović, P.; Tchernychova; E.; Pintar, A. In-situ XAS study of catalytic N_2O decomposition over CuO/CeO_2 catalysts. *ChemCatChem* **2021**, *13*, 1814-1823.
18. Čižmar, T.; Lavrenčič Štangar, U.; Fanetti, M.; Arčon, I. effects of different copper loadings on the photocatalytic activity of TiO_2-SiO_2 prepared at a low temperature for the oxidation of organic pollutants in water. *ChemCatChem* **2018**, *10*, 2982-2993.
19. Teržan, J.; Huš, M.; Arčond, I.; Likozar B.; Djinović, P. Effect of Na, Cs and Ca on propylene epoxidation selectivity over CuO_x/SiO_2 catalysts studied by catalytic tests, in-situ XAS and DFT. *Appl. Surf. Sci*. **2020**, *528*, 146854.
20. Ravel, B.; Newville, M. ATHENA, ARTEMIS, HEPHAESTUS: data analysis for X-ray absorption spectroscopy using IFEFFIT, *J. Synchrotron Radiat*. **2005**, *12*, 537-541.
21. Rehr, J. J.; Albers R. C.; Zabinsky, S. I. High-order multiple-scattering calculations of X-ray absorption fine structure. *Phys. Rev. Lett*. **1992**, *69*, 3397-3400.
22. Žumbar, T.; Arčon, I.; Djinović, P.; Aquilanti, G.; Žerjav, G.; Pintar, A.; Ristić, A.; Dražić, G.; Volavšek, J.; Mali, G.; Popova, M.; Zabukovec Logar, N.; Novak Tušar, N. Winning combination of Cu and Fe Oxide clusters with an alumina support for low-temperature catalytic oxidation of volatile organic compounds. *ACS Appl. Mater. Interfaces* **2023**, *15*, 28747-28762.
23. Gogate, M. R.; Davis, R. J. X-ray Absorption Spectroscopy of a Fe-promoted Rh/TiO_2 catalyst for synthesis of ethanol from synthesis gas. *ChemCatChem* **2009**, *1*, 295-303.
24. Vrbková, E.; Vyskočilová, E.; Rott, M.; Zapletal, M.; Červený, L.;A synthetic route to 4-alkyl-α-methylhydrocinnamylaldehydes. *Res Chem Intermed* **2017**, *43*, 2603–2613.
25. https://foreverest.net/products/extractives-synthetic/helional.html last accesed 17/01/2024
26. Takashi, D.; Yoshihir, Y.; Eiji, S.; Satoru, F.; 2-Methyl-3-(3,4-methylenedioxyphenyl)propanal, and method for production thereof, EP2119713A1, (UBE INDUSTRIES), **2015**.
27. Kroner, A.B.; Newton, M.A.; Tromp, M.; Russell, A.E.; Dent, A.J.; Evans, J. Structural characterization of alumina-supported Rh catalysts: effects of ceriation and zirconiation by using metal-organic precursors. *ChemPhysChem* **2013**, *14*, 3606-3617.
28. Waser, J.; Levy, H.A.; Peterson, S.W. The structure of PdO. *Acta Crystallographica* **1953**, *6*, 661-663.
29. Christy, A.G.; Clark, S.M. Structural behavior of palladium (II) oxide and a palladium suboxide at high pressure: an energy-dispersive X-ray diffraction study. *Phys. Rev., Serie 3. B - Condensed Matter* **1995**, *52*, 9259-9265.
30. Saraev, A.A.; Yashnik, S.A.; Gerasimov, E.Yu.; Kremneva, A.M.; Vinokurov, Z.S.; Kaichev, V.V. Atomic structure of Pd, Pt-, and PdPt-Based catalysts of total oxidation of methane: in situ EXAFS study. *Catalysts* **2021**, *11*, 1446.

31. Matteoli, U.; Beghetto, V.; Scrivanti, A.; Aversa, M.; Bertoldini, M.; Bovo, S.; An Alternative Stereoselective Synthesis of (*R*)- and (*S*)-Rosaphen® via Asymmetric Catalytic Hydrogenation, *Chirality* **2011,** *23*, 779-783.
32. Bovo, S.; Scrivanti, A.; Bertoldini, M.; Beghetto, V., Matteoli, U.; A New Enantioselective Catalytic Route to Florhydral®, *Synth.* **2008**, *16*, 2547-2550.
33. Muravev, V.; Simons, J.F.M.; Parastaev, A.; Verheijen, M.A.; Struijs, J.J. C.; Kosinov, N.; Hensen, E.J. M. Operando spectroscopy unveils the catalytic role of different palladium oxidation states in CO oxidation on Pd/CeO_2 catalysts. *Angew. Chem. Int. Ed.* **2022**, *61*, e202200434.
34. Myers, S.V.; Frenkel, A.I.; Crooks, R.M. X-ray Absorption Study of PdCu bimetallic alloy nanoparticles containing an average of ~64 atoms. *Chem. Mater.* **2009**, 21, 4824-4829.
35. Paula, B. R. S.; Zampieri, D.; Rodrigues, J. A. R.; Moran, P. J. S.; Bioreduction of α-Acetoxymethyl Enones: Proposal for an S_N2' Mechanism Catalyzed by Enereductase *Adv. Synth. Catal*. **2016**, *358*, 3555.
36. Modvig, A.; Andersen, T. L.; Taaning, R. H.; Lindhardt, A.T.; Skrydstrup, T.; Two-Chamber Hydrogen Generation and Application: Access to Pressurized Deuterium Gas. *J. Org. Chem.* **2014**, *79*, 5861–5868.
37. Di Cicco, A.; Aquilanti, G.; Minicucci, M.; Principi, E.; Novello, N.; Cognigni, A.; Olivi, L.; Novel XAFS capabilities at Elettra synchrotron light source, *J. Phys.: Conf. Ser.* **2009**, *190*, 012043.